

BIOINFORMATICS AND BRAIN IMAGING: RECENT ADVANCES AND NEUROSCIENCE APPLICATIONS

Paul M. Thompson, Ph.D.

ABSTRACT

This chapter reviews some exciting new techniques for analyzing brain imaging data. We describe computer algorithms that can discover patterns of brain structure and function associated with Alzheimer's disease, schizophrenia, and normal and abnormal brain development, based on imaging data collected in large human populations. Extraordinary patterns can be discovered with these techniques: dynamic brain maps reveal how the brain grows in childhood, and how it changes in disease, or responds to medication. Genetic brain maps reveal which aspects of brain structure are inherited, shedding light on the nature/nurture debate. They also identify deficit patterns in those at genetic risk for disease. Probabilistic brain atlases now store thousands of these brain maps, models, and images, collected with an array of imaging devices (MRI/fMRI, PET, 3D cryosection imaging, histology). These atlases capture how the brain varies with age, gender, demographics, and in disease. They relate these variations to cognitive, therapeutic, and genetic parameters. With the appropriate computational tools, these atlases can be stratified to create average maps of brain structure in different diseases, revealing unsuspected features. We describe the tools to interact with these atlases. We also review some of the technical and conceptual challenges in comparing brain data across large populations, highlighting some key neuroscience applications.

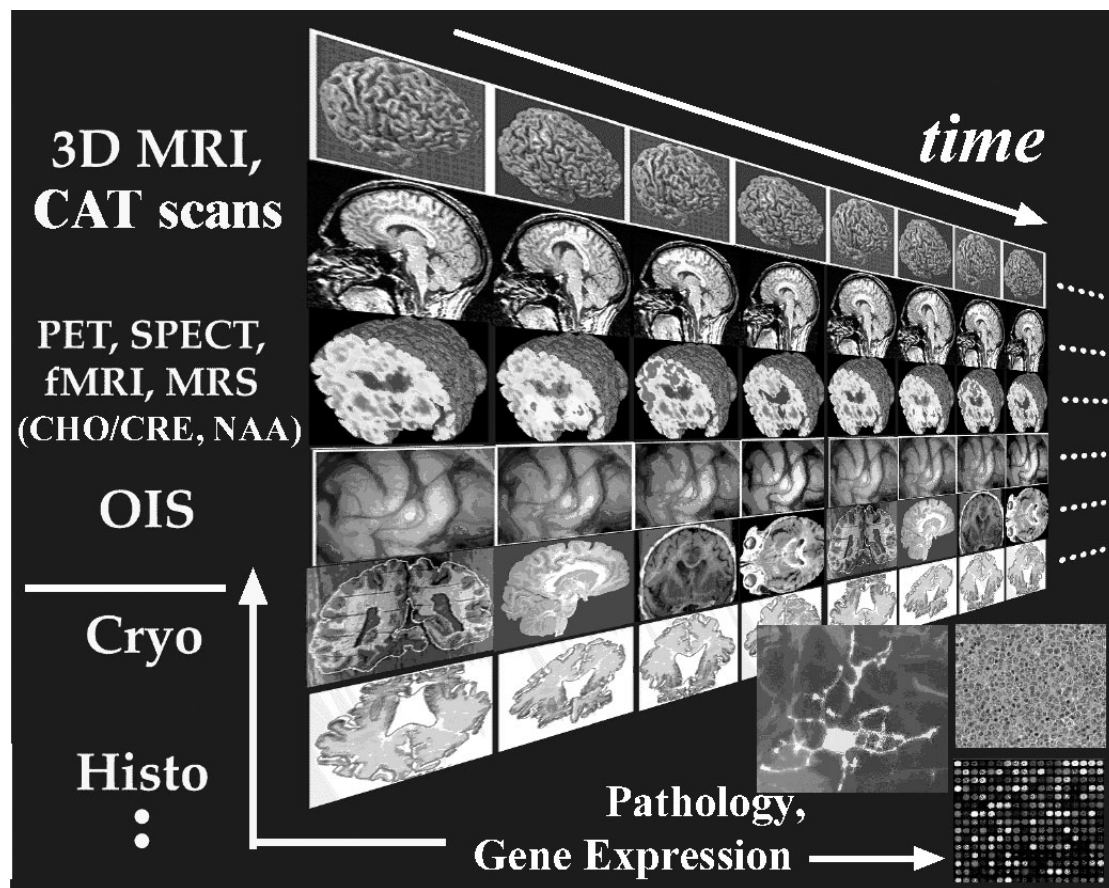
INTRODUCTION

The last few years has seen an explosion in the scope and scale of brain imaging studies. Imaging technology has rapidly advanced (see Fig. 1) and so have the computational methods to analyze images. Patterns of brain structure associated with the major diseases of the brain can be visualized and analyzed. Brain changes over time can be tracked with unprecedented sensitivity, shedding light on development and disease. Dynamic effects of drug treatment on the brain can also be mapped. In the near future, a second revolution in our understanding will come from the merging of large-scale neuroimaging and large-scale genetic studies. These advances will capitalize on sophisticated techniques from both disciplines.

We briefly describe a set of algorithms to detect and visualize effects of disease and genetic factors on the brain. We explain some of the processing steps that occur in a typical neuroscience study, for creating maps and models on the brain. Analysis steps that were recently carried out only on high-performance workstations are now within the reach of most desktop computers. Nonetheless, some computer-intensive analyses involve hundreds or even thousands of subjects. For these, supercomputing technology is increasingly used. Image processing tasks can now be executed over high-speed networks, using client-server pipelines, bringing the power of parallel computers to a desktop machine.

FIGURE 1

Diversity of Brain Maps. Rapid advances in imaging technology have made it possible to create comprehensive maps of brain structure and function, with a broad range of imaging devices, and at a variety of spatial scales. Maps of brain structure are typically based upon 3D tomographic images - magnetic resonance images (MRI), computerized axial tomography (CAT) scans, or anatomic specimens (cryo). A variety of histologic preparations (histo) can also reveal cytoarchitecture and regional molecular content such as myelination patterns, receptor binding sites, protein densities and mRNA distributions. Other brain maps have concentrated on function, quantified by positron emission tomography (PET), functional MRI, optical intrinsic signal imaging (OIS) or electrophysiology. Additional maps have been developed to represent neuronal connectivity and circuitry, based on compilations of empirical evidence. This diverse array of phenotypes will ultimately be correlated with changes in gene expression (bottom right).



BRAIN VARIATIONS

Some challenges in brain imaging are mathematical and statistical as well. Brain structure is extremely complex and variable across subjects. The cerebral cortex, for example, is the target of most functional and structural imaging studies. Nonetheless, gyral patterning variations make it difficult to compare brain data from one individual to another. Neuroimaging studies now typically use mathematics based on random field theory, partial differential equations (PDEs), differential geometry and image processing to encode anatomic or functional variations in a subject group. This disentangles structural and functional differences from normal variations. Below we show some examples where population-specific patterns of cortical organization, asymmetry, and disease-specific trends are resolved that are not apparent in individual brain images.

ALIGNING DATA TO A BRAIN ATLAS

The first step in most structural (or functional) brain imaging analyses is to align individual brain scans to match a standardized template of anatomy, or brain atlas.

BRAIN ATLASES

Brain atlases (e.g. [1,2,3]) provide a structural framework in which individual brain maps can be integrated. Most brain atlases are based on a detailed representation of a single subject's anatomy in a standardized 3D coordinate system, or stereotaxic space. The chosen data set acts as a template on which other brain maps (such as functional images) can be overlaid. The anatomic data provides the additional detail necessary to accurately localize activation sites, as well as providing other structural perspectives such as chemoarchitecture. Digital mapping of structural and functional image data into a common 3D coordinate space is a prerequisite for many types of brain imaging research, as it supplies a quantitative spatial reference system in which brain data from multiple subjects and modalities can be compared and correlated.

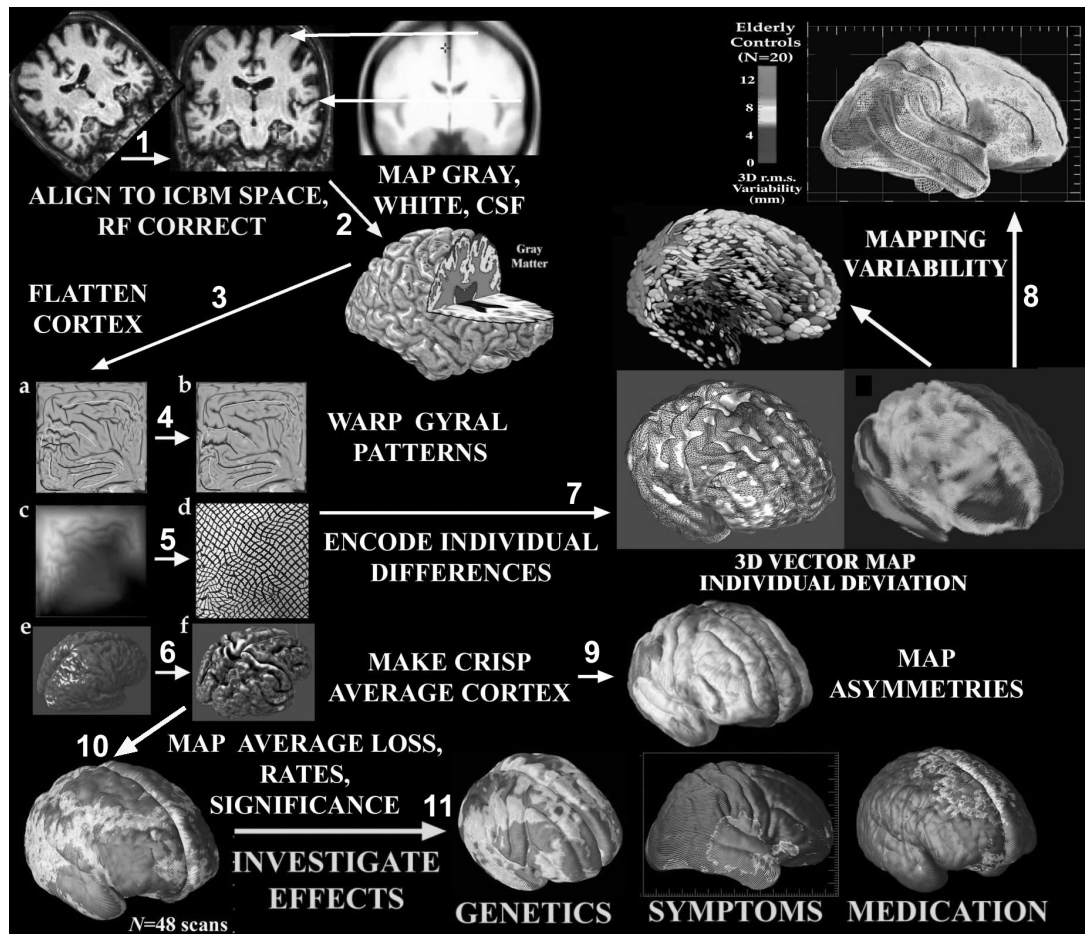
In atlases, spatial normalization systems are typically employed to reference a given brain with an atlas brain [1]. This allows individual data to be superimposed on the data in the atlas - in other words, to be transformed to match the space occupied by the atlas. While stereotaxic methods provide a common coordinate system for pooling activation data and multi-subject comparisons, the accuracy and utility of the atlas is equally dependent on the anatomical template itself [4]. The Talairach atlas was initially widely used in international brain imaging studies. Designed as a coordinate based reference system for neurosurgical studies, the Talairach templates were based on post mortem brain sections from a 60 year-old female subject. This poorly reflects the in vivo anatomy of subjects in activation studies. Atlas plates from orthogonal planes were also inconsistent. To address these limitations, a composite MRI dataset (see Fig. 2; ICBM template) was constructed from young normal subjects whose scans were individually mapped into the Talairach system by linear transformation, intensity normalized, and averaged on a voxel-by-voxel basis [5]. This average intensity template is part of the widely used Statistical Parametric Mapping package (SPM; [6]).

Automated methods can be used to optimally align new MR and PET data with this template (see Fig. 2, step 1). These tune the parameters of the alignment transformation (typically rotations, translations, scales, and shears) to maximize a measure of intensity similarity between the scan being aligned and the target. The similarity measure is typically 3D cross-correlation [7], squared intensity mismatch [8,9], or mutual information [10,11]; (see [12], for practical differences in these approaches).

Any alignment defined for one modality, such as MRI, can be identically applied to another modality, such as PET, if a previous cross-modality intrasubject registration has been performed [8].

FIGURE 2

Creating Brain Maps and Anatomical Models. An image analysis pipeline [12] is shown here. It can be used to create maps that reveal how brain structure varies in large populations, differs in disease, and is modulated by genetic or therapeutic factors. This approach aligns new 3D MRI scans from patients and controls (1) with an average brain template based on a population (here the ICBM template is used, developed by the International Consortium for Brain Mapping [5]). Tissue classification algorithms then generate maps of gray matter, white matter and CSF (2). To help compare cortical features from subjects whose anatomy differs, individual gyral patterns are flattened (3) and aligned with a group average gyral pattern (4). If a color code indexing 3D cortical locations is flowed along with the same deformation field (5), a crisp group average model of the cortex can be made (6), relative to which individual gyral pattern differences (7), group variability (8) and cortical asymmetry (9) can be computed. Once individual gyral patterns are aligned to the mean template, differences in gray matter distribution or thickness (10) can be mapped, pooling data from homologous regions of cortex. Correlations can be mapped between disease-related deficits and genetic risk factors (11). Maps may also be generated visualizing linkages between deficits and clinical symptoms, cognitive scores, and medication effects.



POPULATION-BASED ATLASES

After aligning data into a stereotaxic coordinate space, anatomical structures can be referred to in standardized coordinates. Digital models of brain structures can also be built, and their boundary coordinates stored as a list of 3D locations in stereotaxic space. These coordinates provide an international standard for reporting imaging findings, such as functional activation sites, or maps of structural differences. However, even in stereotaxic space, brain structures vary from one individual to another in every metric: shape, size, complexity, and orientations relative to one another. To help understand this variation and resolve typical anatomic patterns, it would be ideal if an average representation of brain structure could be developed for a particular subject group, such as patients with dementia or schizophrenia. Normal anatomic variations relative to this average could then be encoded statistically, and used to map regions of significant abnormality in disease. Probabilistic brain atlases

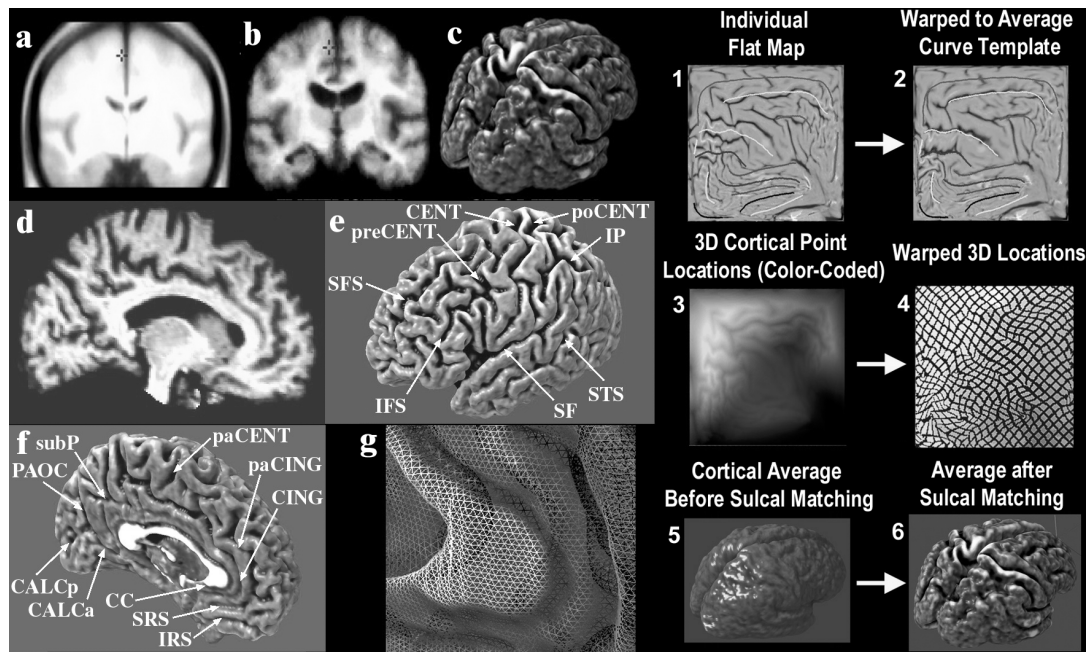
[2,14,15] perform this task. They store information on individual differences, in a computational format that reveals where variation is greatest and what factors contribute to it. The process of encoding these anatomic variations is described next.

BRAIN AVERAGING

Consider the challenges in creating a typical, or 'average', model of brain structure. If the image intensities of a group of subjects' MRI scans are averaged together, pixel-by-pixel, cortical features are washed away due to anatomical variability in the population (Fig. 3(a)). Fig. 3 illustrates a more sophisticated method to create a well-resolved, average template of anatomy (Fig. 3(b) and (c) show an average brain template based on N=9 Alzheimer's patients). Here group features are reinforced in their mean anatomic locations ([16]; Fig. 3, panel 6). This method, based on a technique called cortical pattern matching [17-20], can also generate average maps of gyral pattern asymmetry, and gray matter deficits a group, pinpointing disease-specific patterns (Fig. 5). Importantly, detailed information is retained on individual variability (Fig. 4(c),(d)). This is useful for understanding genetic influences on brain structure (see later). We describe how these individual differences are measured next.

FIGURE 3

Creating 3D Average Brain Templates for a Population. Before computing individual anatomical differences, it is useful to create an average model of anatomy for a specific population. If MRI scans from a group of subjects are mutually aligned and their intensities are averaged together pixel-by-pixel [(a); [5]], cortical features are washed away. To retain these features in the group average [(b),(c)], a procedure called cortical pattern matching can be used (see [15] for details). From each individual's MRI scan (d) a cortical model [(e),(f)] consisting of discrete triangular elements (g) is created and flattened (panel 1), along with digital models of cortical sulci traced on the brain surface. A warping field drives the flat map (1), and a color code indexing corresponding 3D cortical positions (3),(4), to match an average set of flat 2D sulcal curves (2). If these color images are averaged across subjects and decoded before cortical pattern matching (3), a smooth average cortex (5) is produced. If they are warped first (4), averaged, and decoded, a crisp average cortex appears in which anatomical features are reinforced and appear in their mean stereotaxic locations (6). Such cortical averages provide a standard template relative to which individual differences may be measured (Fig. 4). Using warping (4), cortical data can be transferred, from individuals whose anatomy is different, onto a common anatomic template for comparison and integration.



CORTICAL PATTERN MATCHING AND ANATOMICAL AVERAGING

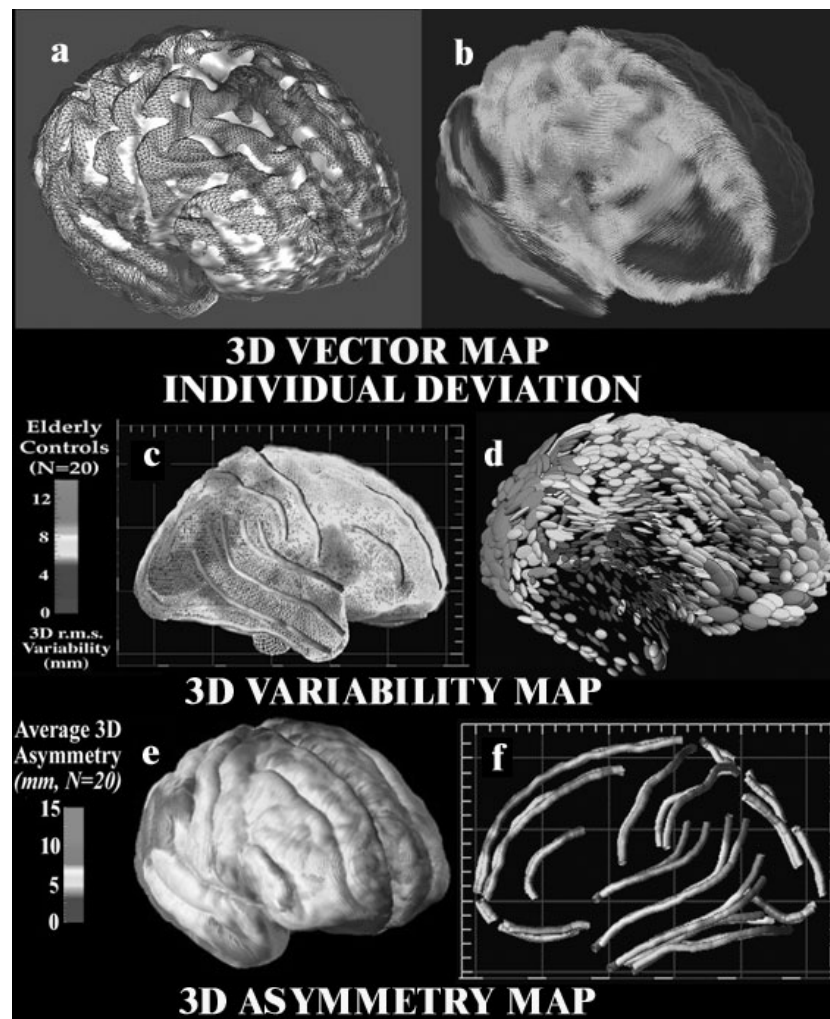
In high-quality MRI data (typically 1x1x1 mm image resolution and good tissue contrast is required), it is relatively easy to extract a 3D cortical surface model (Fig. 3(e),(f)) from an individual subject's scan (Fig. 3(d)). This represents their cortical surface anatomy in detail (Fig. 3(g); triangulated mesh). A set of 38 sulcal curves (Fig. 3(e),(f)) is then manually traced, representing each subject's primary gyral pattern. These curves are used as anchors to create a deformation mapping (Fig. 3, panel 2), which distorts the anatomy of one subject onto another, matching sulcal features exactly. To compute this mapping, cortical models and curves are first flattened (Fig. 3, panel 1), and a flow field is computed in the flattened space, to drive individual sulcal features onto an average set of curves (panel 2). Using a mathematical trick, a color code representing 3D locations of cortical points in each subject (panel 3) is convected along with this flow (panel 4). Then these warped color images are averaged across subjects and decoded to produce a crisp average cortical model for the group (panel 6).

MEASURING INDIVIDUAL BRAIN DIFFERENCES

These deformation maps represent the complex distortion required to match one cortex to a group average (Fig. 4(a),(b)). They also store local information on individual differences in gyral patterns. In a normal population, the amount of variability can be mapped by converting these differences into local measures of variance (3D r.m.s. deviation from the average anatomy). Gyral pattern variation is found to be greatest in perisylvian language-related cortices (red colors, Fig. 4(c)). Directional biases in gyral pattern variation can also be visualized (elongated ellipsoids, Fig. 4(d)). Group features of anatomy also emerge that are not apparent in individual subjects. The atlas localizes a prominent asymmetry in perisylvian cortices: right hemisphere structures are, on average, torqued forward relative to their counterparts on the left ([21]; see Fig. 4(e),(f)).

FIGURE 4

Measuring Individual Brain Differences and Population Variability. When a individual brain (brown mesh, (a)) is globally aligned and scaled to match a group average cortical model (white surface), a 3D deformation is computed to match its gyral anatomy with the group average (pink colors: large deformations, (b)). The 3D root mean square magnitude of these deformation vectors (variability map, (c)) shows that gyral pattern variability is greatest in perisylvian language areas (red colors). 3D confidence regions for gyral variations can be also stored locally to detect cortical abnormalities ((d), [14]). Ellipsoids, (d), are elongated along directions in which normal variation is greatest; pink colors denote greatest anatomic variation. Deformations that match the gyral anatomy of one hemisphere with a reflected version of the opposite hemisphere can be averaged across subjects to detect anatomic asymmetries. These are greatest in perisylvian cortices (red colors, (e),(f); [13]; Geschwind and Levitsky [21] first observed this feature in a volumetric study). All these maps provide detailed structural phenotypes that can be mined for genetic influences. The maps shown here are based on a group of 20 healthy elderly subjects, but can be recomputed for any population.



GRAY MATTER DIFFERENCES

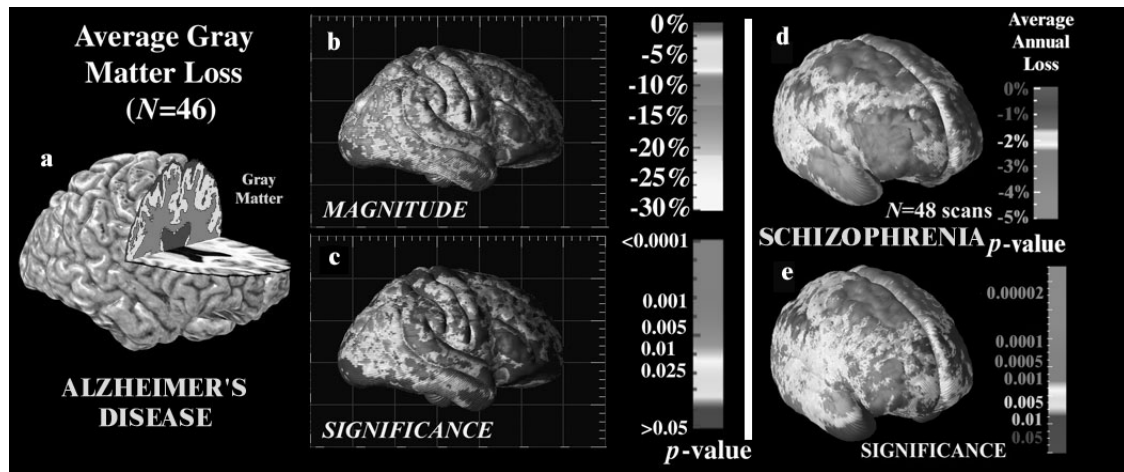
Among the structural features that are genetically regulated and have implications for cortical function is the distribution of gray matter across the cortex. This varies widely across normal individuals, with developmental waves of gray matter gain and loss subsiding by adulthood [22,23]. Complex deficit patterns are observed in Alzheimer's disease, schizophrenia [24,13], and healthy subjects at genetic risk for these disorders [25]. Figure 3 shows the average profile of gray matter deficits in early Alzheimer's disease, based on MRI data from 26 AD patients and 20 healthy controls. To produce these maps, a tissue classifier creates maps of gray matter (green colors, Fig. 5(a)) in each subject. This type of algorithm separates the voxels of an MRI scan into gray matter, white matter, and CSF, and a background (non-brain) class, typically by computing parameters of their intensity distributions. Rather than compute cortical thickness, which is extremely difficult in MRI data, a related measure, termed 'gray matter density' is more commonly used [26,24,9]. This describes the proportion of pixels segmenting as gray matter in a small spherical region around each cortical point. By storing individual variations in gray matter density at each cortical point, differences between the diseased group and the healthy control group can be expressed as a percentage deficit, or as a significance map (Fig. 5(c)). Significance maps report the results of a statistical test, assessing the evidence for a group difference, at each cortical point; they plot these results in color as a color-coded map. An advantage of this approach relative to volumetric studies is the ability to localize effects on brain structure in the form of a map. When trying to detect systematic effects on brain structure, cortical pattern matching also increases signal to noise by associating gray matter measures from corresponding cortical regions; this also adjusts for shape changes in longitudinal studies (Fig. 5(d),(e)). In the resulting maps, regions of comparatively spared tissue may appear sharply delimited from regions with significant loss (Fig. 5(b)) or progressive loss (Fig. 5(d),(e)).

GENETIC INFLUENCES ON BRAIN STRUCTURE

Specialized methods have also been developed to assess how genes and environment affect brain function. Typically the goal is to shed light on the mechanism and transmission of disease, or to help understand the effects of genes and environmental factors on cognitive skills and behavior. Brain mapping methods to assess individual differences can also be applied to help test behavioral genetic models of individual variation. Rather than display statistics that describe the significance of disease effects on brain structure, genetic models typically describe the proportion of variability in brain structure that is due to genetic factors, environmental factors, or their interaction (see [27] for a review). Estimated model parameters, their error variance, and their goodness of fit (e.g. c^2) may also be displayed as color-coded maps, as well as simpler measures of intraclass correlations and heritability coefficients, which are described next.

FIGURE 5

Mapping Gray Matter Deficits in a Population. Measures of gray matter (a) can be computed from MRI scans and compared across individuals and groups. Data from corresponding cortical regions are compared using cortical pattern matching (Fig. 3). Patients with mild to moderate Alzheimer’s disease show a severe loss of gray matter [(b),(c)] relative to matched healthy controls, especially in temporal cortices (where deficits approach 30% locally – red colors). Patients with childhood onset schizophrenia show a progressive loss of gray matter, especially in temporal and superior frontal cortices [(d),(e)]. These structural measures are tightly correlated with worsening symptoms [18,28], offering a promising endophenotype (biological marker) for genetic studies. These biological markers are likely to be more directly influenced by genes coding for structural proteins, regulatory elements, and signaling molecules, than clinical symptoms, such as hallucinations or disordered thinking.



GENETIC BRAIN MAPS

Fig. 6 shows the intraclass correlations in gray matter (Fig. 6, left columns) in groups of monozygotic (MZ) and dizygotic (DZ) twins. Note that this type of map captures individual differences. In a sense it is the opposite of the group average maps, which map patterns that characterize a group overall. These maps were computed as part of a study to determine genetic influences on brain structure [29,27,30]. Genetic influences on any trait are typically estimated by measuring similarities among relatives with different degrees of genetic affinity. Here the measured trait is gray matter distribution, but the methods are the same as those for estimating the heritability of height, weight, or a particular disease such as schizophrenia or autism. In the classical twin design, a feature is regarded as heritable if it shows a genetic cascade in which within-pair correlations (typically called intraclass correlations, or ICCs) are higher for pairs of MZ twins (who share all their genes, except for rare somatic mutations), and lower for same-sex DZ twin pairs (who on average share half their genes). Falconer's method [31] computes heritability as twice the difference between these correlations. High values, near 1.0, are found for the most genetically determined traits, and near-zero values for traits that are unaffected by individual genetic differences. MZ within-pair gray matter differences are almost zero (intraclass $r \sim 0.9$ and higher, $p < 0.0001$ corrected; Fig. 6, left column) in a broad anatomical band encompassing frontal, sensorimotor and linguistic cortices, including Broca's speech and Wernicke's language comprehension areas. Since MZ twins are genetically identical (except for rare somatic mutations), any regional differences are attributed to environmental effects or gene-environment interactions. The maps show how sensorimotor and parietal occipital, but not frontal, territory is significantly more similar in DZ twins than random pairs. Affinity is greatest in the MZ pairs, suggesting a genetic continuum in the determination of structure. Middle frontal regions, in the vicinity of Brodmann areas 9 and 46, displayed a 90-95% genetic determination of structure (i.e., $h^2 \sim 0.90-$

0.95). Many regions are under tight genetic control (bilateral frontal and sensorimotor regions, $p < 0.0001$; Fig. 6; right column), and heritability estimates are comparable with twin-based estimates for the most highly genetically-determined human traits, including fingerprint ridge count ($h^2 = 0.98$), height ($h^2 = 0.66-0.92$), and systolic blood pressure ($h^2 = 0.57$).

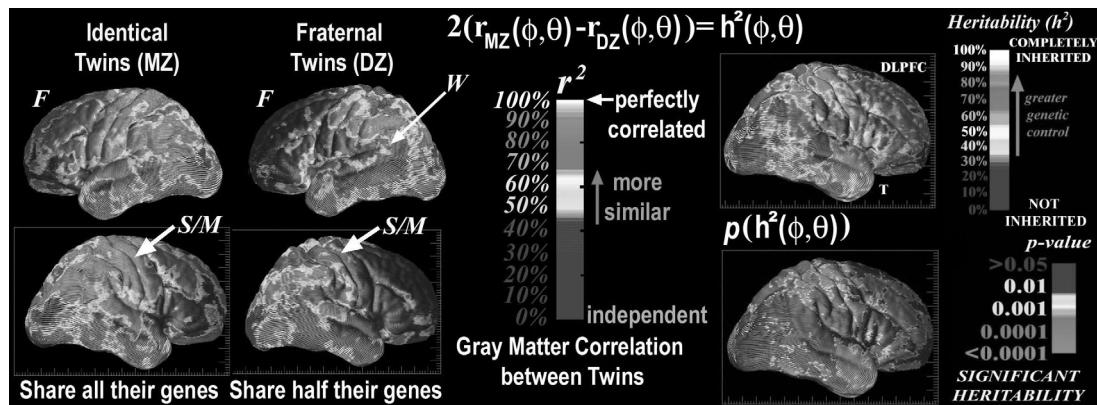
PERMUTATION TESTING

The significance of these statistical genetic brain maps, and the previous maps of disease effects, is typically assessed using either parametric or nonparametric methods. In each case appropriate adjustments must be made for multiple comparisons, as is conventional in functional brain imaging (see [12] for current approaches). These adjustments note that thousands of statistical tests are performed at different points on the brain surface, but they are certainly not independent tests, as their results are highly spatially correlated. Typically, to assess whether an observed pattern of

statistics or significance values could have occurred by accident, a Monte Carlo simulation is run in which subjects are randomly assigned to groups. A null distribution is then assessed for the statistic of interest, and the chance of accidentally finding the pattern that occurred in the experiment is assessed [12]. These operations are computer-intensive, and their power is not optimal. The development of analytical formulas for statistical distributions on manifolds is therefore an active topic of research, and is likely to empower future brain mapping studies [12,32].

FIGURE 6

Mapping Genetic Influences on Brain Structure: Heritability Maps. Color-coded maps (left columns) show local gray matter correlations between MZ and DZ twins. Falconer's heritability formula [31] is applied to data from corresponding cortical regions (within and across twin pairs). The resulting value of h^2 , and its significance (lower right panel) is plotted at each cortical point. Note the significant genetic control in an anatomical band encompassing parietal, sensorimotor, and frontal cortices.



DYNAMIC BRAIN MAPS

Everyone's brain shrinks with age, and not in a uniform way. Diseases such as Alzheimer's cause changes in the overall rates, and patterns, of brain change. Population-based atlases can store key statistics on the rates of these brain changes. These are especially relevant to the understanding of development [33] as well as relapsing-remitting diseases such as multiple sclerosis and tumor growth [34,35]. They also provide normative criteria for early brain change in patients with dementia [36,37,13], with mild cognitive impairment [38], or in those at genetic risk for Alzheimer's disease [39]. An interesting application is the compilation of dynamic maps to characterize brain growth in development or degenerative change, which we illustrate next.

TENSOR MAPS OF BRAIN CHANGE

Maps of brain change over time can be created based on a deformation mapping concept. In this approach, a 3D elastic deformation is calculated (Fig. 7). This deformation, or warping field, drives an image of a subject's anatomy at a baseline timepoint to match its shape in a later scan. Dilation and contraction rates, and even the principal directions of growth, are derived by examining the eigenvectors of the deformation gradient tensor, or the local Jacobian matrix of the transform that maps the earlier anatomy onto the later one. Applications include the mapping of brain growth patterns in children [40], measuring tumor response to novel chemotherapy agents [34], and the mapping of degenerative rates in Alzheimer's disease (Fig. 7). By building probability densities on registered tensor fields (e.g. [40]), a quantitative framework can be used to detect normal and aberrant brain change, and how medication affects these changes in clinical trials (see [16] for a review).

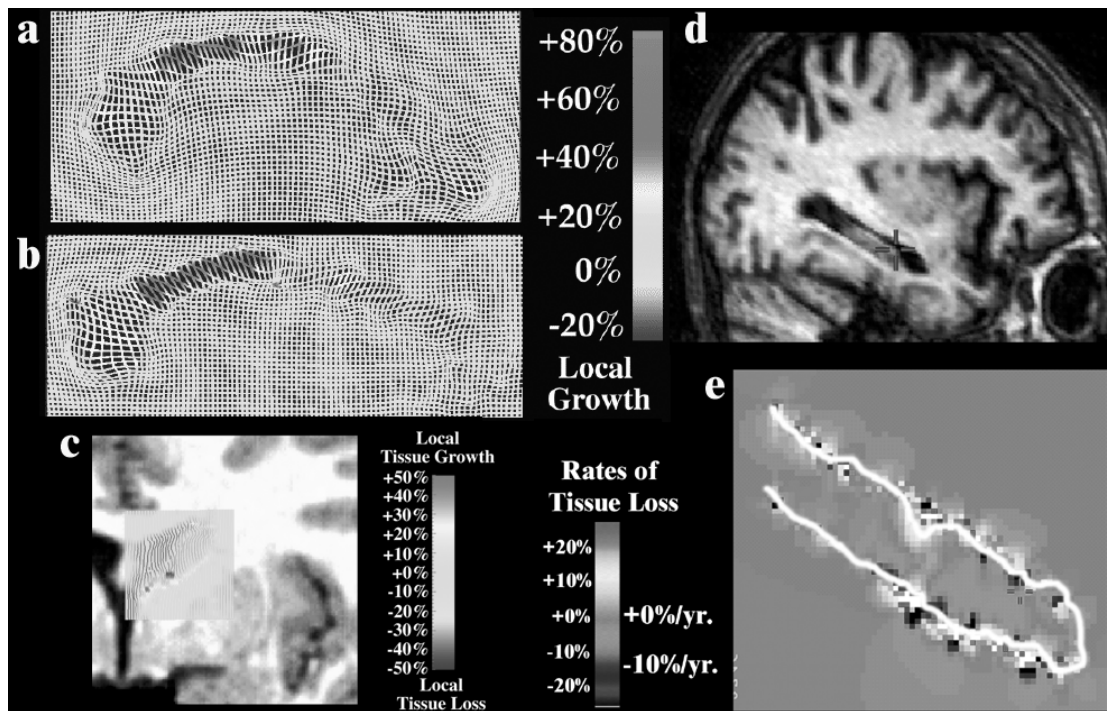
CONCLUSION

There are numerous implementations and applications of brain maps to study morphology. Each new approach in brain morphology has the capacity to measure, visualize, compare and summarize brain images. There are many varieties, from descriptions of structure to function of the whole brain to maps of groups or populations. Maps enable comparison across individuals, modalities or states. While dependent upon

appropriate coordinate systems, deformation methods and visualization strategies, accurate and representative brain maps hold enormous promise for helping to create a comprehensive understanding of brain in health and disease. The merger of methods from imaging and genetics is likely to expedite a second revolution in our understanding of the brain.

FIGURE 7

Tensor Maps of Brain Change: Visualizing Growth and Atrophy. If follow-up (longitudinal) images are available, the dynamics of brain change can be measured with tensor mapping approaches [40]. These map volumetric change at a local level, and show local rates of tissue growth or loss. Fastest growth is detected in the isthmus of the corpus callosum in two young girls identically scanned at ages 6 and 7 (a), and at ages 9 and 13 (b). Maps of loss rates in tissue can be generated for the developing caudate ((c), here in a 7-11 year old child), and for the degenerating hippocampus [(d), (e)]. In (e), a female patient with mild Alzheimer’s disease was imaged at the beginning and end of a 19 month interval with high-resolution MRI. The patient, aged 74.5 years at first scan, exhibits faster tissue loss rates in the hippocampal head (10% per year, during this interval) than in the fornix. These maps can help elucidate the dynamics of therapeutic response in an individual or a population [18,34].



ACKNOWLEDGMENTS

This work was generously supported by research grants from the National Library of Medicine (LM/MH05639), NCRR (RR13642), and by a Human Brain Project grant known as the International Consortium for Brain Mapping, which is funded jointly by NIMH and NIDA (P20 MH/DA52176). Special thanks go to Arthur Toga, Tyrone Cannon, Judith Rapoport, Jay Giedd, Michael Mega, Christine Vidal, Kira Hayashi, Katherine Narr, Roger Woods, Elizabeth Sowell, John Mazziotta, David MacDonald, Alan Evans, Greig de Zubicaray, Andrew Janke, and the members of the UCLA Laboratory of Neuro Imaging for their work and support in these studies. We also thank Jaakko Kaprio and his colleagues for their collaborative work on our twin project.

FURTHER READING

Genes, Brain, and Cognition

http://www.loni.ucla.edu/~thompson/MEDIA/NN/Press_Release.html

Mapping Brain Growth in Children

http://www.loni.ucla.edu/~thompson/MEDIA/press_release.html

Brain Mapping in Schizophrenia

http://www.loni.ucla.edu/~thompson/MEDIA/PNAS/Press_release.html

REFERENCES

1. Talairach J, Tournoux P (1988). *Co-planar Stereotaxic Atlas of the Human Brain*, New York: Thieme.
2. Mazziotta JC, Toga AW, Evans AC, Fox P, Lancaster J (1995) A Probabilistic Atlas of the Human Brain: Theory and Rationale for its Development, *NeuroImage* 2: 89-101.
3. Kikinis R, Shenton ME, Iosifescu DV, McCarley RW, Saiviroonporn P, Hokama HH, Robatino A, Metcalf D, Wible CG, Portas CM, Donnino R, Jolesz F (1996). A Digital Brain Atlas for Surgical Planning, Model-Driven Segmentation, and Teaching, *IEEE Trans. on Visualization and Comp. Graphics*, Sept. 1996, 2(3):232-241.
4. Roland PE, Zilles K. The developing European computerized human brain database for all imaging modalities. *Neuroimage*. 1996 Dec;4(3 Pt 2):S39-47.
5. Evans AC, Collins DL, Neelin P, MacDonald D, Kamber M, Marrett TS (1994). Three-Dimensional Correlative Imaging: Applications in Human Brain Mapping, in: *Functional Neuroimaging: Technical Foundations*, Thatcher RW, Hallett M, Zeffiro T, John ER, Huerta M [eds.], 145-162.
6. Friston KJ, Holmes AP, Worsley KJ, Poline JP, Frith CD, Frackowiak RSJ (1995). Statistical Parametric Maps in Functional Imaging: A General Linear Approach, *Human Brain Mapping* 2:189-210.
7. Collins DL, Holmes CJ, Peters TM, Evans AC (1995). Automatic 3D Model-Based Neuroanatomical Segmentation, *Human Brain Mapping* 3:190-208.
8. Woods RP, Grafton ST, Watson JDG, Sicotte NL, Mazziotta JC (1998). Automated image registration: II. Intersubject validation of linear and nonlinear models. *J. Computer Assisted Tomography* 1998.
9. Ashburner J, Friston KJ. Voxel-based morphometry--the methods. *Neuroimage* 11, 6:805-21 (2000).
10. Viola PA, Wells WM (1995). Alignment by Maximization of Mutual Information, 5th IEEE Int. Conf. on Computer Vision, 16-23, Cambridge, MA.
11. Wells WM, Viola P, Atsumi H, Nakajima S, Kikinis R (1997). Multi-Modal Volume Registration by Maximization of Mutual Information, *Medical Image Analysis* 1(1):35-51.
12. Thompson PM et al., *Brain Image Analysis and Atlas Construction*, in: Fitzpatrick M, Sonka M (ed.), *Handbook on Medical Image Analysis*, SPIE Press (2000).
13. Thompson PM, Mega MS, Vidal C, Rapoport JL, Toga AW (2001). Detecting Disease-Specific Patterns of Brain Structure using Cortical Pattern Matching and a Population-Based Probabilistic Brain Atlas, *IEEE Conference on Information Processing in Medical Imaging (IPMI)*, UC Davis, 2001, in: *Lecture Notes in Computer Science (LNCS)* 2082:488-501, M Insana, R Leahy [eds.], Springer-Verlag.
14. Thompson PM, MacDonald D, Mega MS, Holmes CJ, Evans AC, Toga AW (1997). Detection and Mapping of Abnormal Brain Structure with a Probabilistic Atlas of Cortical Surfaces, *J. Comp. Assist. Tomogr.* 21(4):567-581, Jul.-Aug. 1997.
15. Thompson PM, Woods RP, Mega MS, Toga AW. Mathematical/computational challenges in creating deformable and probabilistic atlases of the human brain. *Human Brain Mapping* 9(2):81-92 (2000).
16. Thompson PM, Toga AW (2002). A Framework for Computational Anatomy [Invited Paper],

- Computing and Visualization in Science, 5:1-12.
17. Thompson PM, Toga AW (1996). A Surface-Based Technique for Warping 3-Dimensional Images of the Brain, *IEEE Transactions on Medical Imaging*, Aug. 1996, 15(4):1-16.
 18. Thompson PM, Hayashi KM, de Zubicaray G, Janke AL, Rose SE, Semple J, Doddrell DM, Cannon TD, Toga AW (2002). Detecting Dynamic and Genetic Effects on Brain Structure using High-Dimensional Cortical Pattern Matching, *Proc. International Symposium on Biomedical Imaging (ISBI2002)*, Washington, DC, July 7-10, 2002.
 18. Thompson PM, Vidal CN, Giedd JN, Gochman P, Blumenthal J, Nicolson R, Toga AW, Rapoport JL (2001). Mapping Adolescent Brain Change Reveals Dynamic Wave of Accelerated Gray Matter Loss in Very Early-Onset Schizophrenia, *Proceedings of the National Academy of Sciences of the USA*, 98(20):11650-11655, September 25, 2001.
 19. Davatzikos C (1996). Spatial Normalization of 3D Brain Images using Deformable Models, *J. Comp. Assisted Tomography* 20(4):656-665, Jul.-Aug. 1996.
 20. Fischl B, Sereno MI, Tootell RBH, Dale AM (1999). High-Resolution Inter-Subject Averaging and a Coordinate System for the Cortical Surface, *Hum Brain Mapp.* 1999;8(4):272-84.
 21. Geschwind N, Levitsky W. Human brain: left-right asymmetries in temporal speech region. *Science*. 1968 Jul 12;161(837):186-7. Geschwind DH, Miller BL, DeCarli C, Carmelli D. Heritability of lobar brain volumes in twins supports genetic models of cerebral laterality and handedness. *Proc Natl Acad Sci U S A*. 2002 Mar 5;99(5):3176-81.
 22. Sowell ER et al. In vivo evidence for post-adolescent brain maturation in frontal and striatal regions. *Nat. Neurosci.* 2,10:859-61 (1999).
 23. Giedd JN et al. Brain development during childhood and adolescence: a longitudinal MRI study. *Nat. Neurosci.* 2,10:861-3 (1999).
 24. Thompson PM et al. Cortical change in Alzheimer's disease detected with a disease-specific population-based brain atlas. *Cerebral Cortex* 11, 1-16 (2001).
 25. Cannon TD, Thompson PM, van Erp T, Toga AW, Poutanen V-P, Huttunen M, Lönngqvist J, Standertskjöld-Nordenstam C-G, Narr KL, Khaledy M, Zoumalan CI, Dail R, Kaprio J (2002). Cortex Mapping Reveals Regionally Specific Patterns of Genetic and Disease-Specific Gray-Matter Deficits in Twins Discordant for Schizophrenia, *Proceedings of the National Academy of Sciences of the USA*, vol. 99, no. 5: 3228-3233, February 26, 2002.
 26. Wright IC et al. A voxel-based method for the statistical analysis of gray and white matter density applied to schizophrenia. *Neuroimage* 2, 4:244-52 (1995).
 27. Thompson PM, Cannon TD, Toga AW (2002). Mapping Genetic Influences on Human Brain Structure [Review], *Annals of Medicine*, 2002.
 28. Thompson PM, Mega MS, Toga AW (2000). Disease-Specific Brain Atlases, Invited Chapter in: *Brain Mapping: The Disorders*, Toga AW, Mazziotta JC [eds.], Academic Press, July 2000.
 29. Thompson PM, Cannon TD, Narr KL, van Erp T, Khaledy M, Poutanen V-P, Huttunen M, Lönngqvist J, Standertskjöld-Nordenstam C-G, Kaprio J, Dail R, Zoumalan CI, Toga AW (2001). Genetic Influences on Brain Structure, *Nature Neuroscience* 4(12):1253-8, Dec. 2001.
 30. Plomin R, Kosslyn SM (2001). Genes, brain and cognition. *Nature Neuroscience* 4(12):1153-4.
 31. Falconer DS. *Introduction to Quantitative Genetics*, Longman, Essex, UK, ed. 3 (1989).
 32. Taylor JE, Adler RJ. Euler characteristics for Gaussian fields on manifolds

- <http://www.math.mcgill.ca/jtaylor/publications/index.html> (2002).
33. Lange N, Giedd JN, Castellanos FX, Vaituzis AC, Rapoport JL (1997). Variability of human brain structure size: ages 4-20 years.
 34. Haney S, Thompson PM, Cloughesy TF, Alger JR, Frew A, Torres-Trejo A, Mazziotta JC, Toga AW (2001). Mapping Response in a Patient with Malignant Glioma, *J. Computer Assisted Tomography*, 2001.
 35. Haney S, Thompson PM, Cloughesy TF, Alger JR, Toga AW (2001). Tracking Tumor Growth Rates in Patients with Malignant Gliomas: A Test of Two Algorithms, *American Journal of Neuroradiology (AJNR)* 22(1):73-82, Jan. 2001.
 36. Jernigan TL, Archibald SL, Fennema-Notestine C, Gamst AC, Stout JC, Bonner J, Hesselink JR (2001). Effects of age on tissues and regions of the cerebrum and cerebellum. *Neurobiol Aging*. 2001 Jul-Aug;22(4):581-94.
 37. Janke AL, Zubicaray Gd, Rose SE, Griffin M, Chalk JB, Galloway GJ (2001). 4D deformation modeling of cortical disease progression in Alzheimer's dementia. *Magn Reson Med*. 2001 Oct;46(4):661-6.
 38. Studholme C, Cardenas V, Schuff N, Rosen H, Miller B, Weiner MW (2001). Detecting Spatially Consistent Structural Differences in Alzheimer's and Fronto Temporal Dementia Using Deformation Morphometry. *MICCAI* 2001, 41-48.
 39. Small GW, Ercoli LM, Silverman DH, Huang SC, Komo S, et al. Cerebral metabolic and cognitive decline in persons at genetic risk for Alzheimer's disease. *Proc Natl Acad Sci U S A*. 2000 May 23;97(11):6037-42.
 40. Thompson PM, Giedd JN, Woods RP, MacDonald D, Evans AC, Toga AW (2000). Growth Patterns in the Developing Brain Detected By Using Continuum-Mechanical Tensor Maps, *Nature*, 404:(6774) 190-193, March 9, 2000.

